Heteroatom Chemistry
Volume 19, Number 4, 2008

Thiol–Thione Tautomeric Forms Recognition on the Example of 4-[3-(2-Methyl-furan-3-yl)-5-thioxo-1,2,4-triazolin-4-yl]acetic Acid

Agata Siwek,[1] Monika Wujec,[1] Irena Wawrzycka-Gorczyca,[2] Maria Dobosz,[1] and Piotr Paneth[3]

[1]*Department of Organic Chemistry, Faculty of Pharmacy, Medical University, Staszica 6, 20-081 Lublin, Poland*

[2]*Department of Crystallography, Faculty of Chemistry, Maria Curie-Sklodowska University, Maria Curie-Sklodowska 3, 20-031 Lublin, Poland*

[3]*Institute of Applied Radiation Chemistry, Technical University of Lodz, Zeromskiego 116, 90-924 Lodz, Poland*

Received 26 July 2007; revised 22 December 2007

ABSTRACT: *The synthesis of 4-[3-(2-methyl-furan-3-yl)-5-thioxo-1,2,4-triazolin-4-yl]acetic acid, its structural study in the solid state, and the thiol–thione tautomeric recognition on the basis of spectroscopic data and theoretical calculations are presented. It is shown that NMR spectra, especially ^{13}C and ^{15}N, are indicative of the actual tautomeric form whereas vibrational data can be ambiguous.*
 Heteroatom Chem 19:337–344, 2008; Published online in Wiley InterScience (www.interscience.wiley.com). DOI 10.1002/hc.20433

INTRODUCTION

The synthesis of mercapto-functionalized azoles proved particularly an attractive route to substituted azoles of pharmacological importance [1]. Mercapto-azoles can exist in two major tautomeric forms that exhibit different reactivities, as demonstrated for polymerization processes, metal complexation, and substitution reactions [1b,1d,2]. The thiol–thione (and also selenol–selone [3]) tautomerism of these compounds remains a point of controversy, because it is not straightforward to determine which of the two forms is present, that is, 1-methyl-2-mercaptoimidazole/1-methylimidazole-2-thione is known as methimazole—the name given to evade the description of the actual tautomeric form. Similar situation occurs for mercapto-triazoles (Fig. 1). Whereas most of the authors have suggested that the thione form is dominant in the solid state and in a neutral solution [2b,4], the presence of the thiol form has also been proposed [5]. The role of solvent molecules in shifting the equilibrium toward thione form has been pointed out recently [6]. During our recent synthetic studies on more than 260 mercapto-azoles [7], we have carried out X-ray analysis for a few selected compounds that were prone to crystallization. All of these compounds were crystallized to

Correspondence to: Agata Siwek; e-mail: agata.siwek@am.lublin.pl.

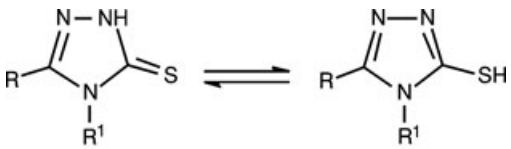

FIGURE 1 Thiol–thione forms of 3,4-disubstituted-Δ^{2-}1,2,4-triazoline-5-thiones.

the thione form. Among these were newly synthesized mercapto-triazole and 4-[3-(2-methyl-furan-3-yl)-5-thioxo-1,2,4-triazolin-4-yl]acetic acid (**1**). Theoretical calculations have shown that for this compound the energy gap between the thione and thiol forms is the largest among those studied. We have, therefore, selected **1** for the comprehensive structural study after combining vibration spectroscopy, X-ray studies, and theoretical analysis in the hope to provide a deeper insight into the differences between the thiol and thione tautomers of mercapto-triazoles and to identify the analytical methods that are most likely to differentiate them.

RESULTS AND DISCUSSION

4-[3-(2-Methyl-furan-3-yl)-5-thioxo-1,2,4-triazolin-4-yl]acetic acid (**1**) was synthesized according to the method shown in Scheme 1 and was confirmed by the X-ray analysis that it is a thione tautomer. Its spectroscopic properties, determined experimentally as well as theoretically, are presented and are compared with the corresponding properties calculated for its thiol form.

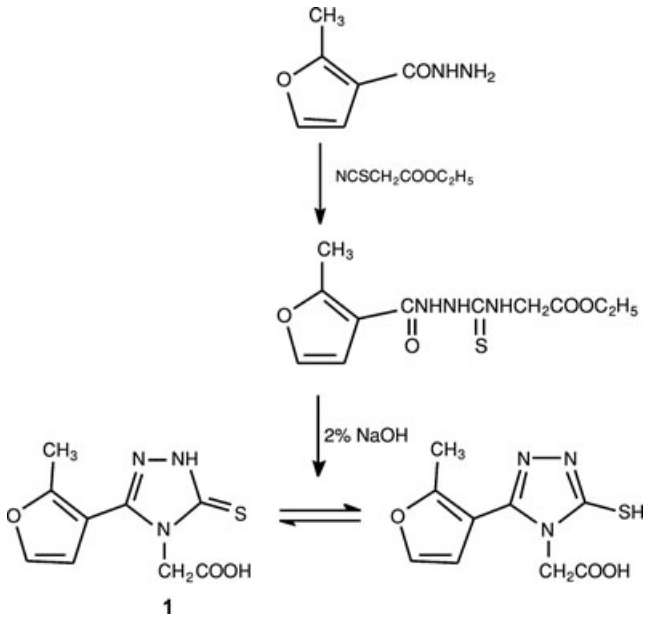

SCHEME 1 Synthesis of 4-[3-(2-methyl-furan-3-yl)-5-thioxo-1,2,4-triazolin-4-yl]acetic acid (**1**).

Crystal Structure

The determined molecular structure of **1** and the atom-numbering scheme, used throughout in this article, is shown in Fig. 2. Crystal data indicated monoclinic $C_9H_7N_3O_3S$ structure with the space group $P2_1/c$, $a = 6.466(1)$, $b = 14.845(3)$, $c = 11.004(2)$ Å, $\beta = 94.43(3)^\circ$, $V = 1053.1(3)$ Å^3, $Z = 4$, $d_x = 1.496$ g cm^{-1}.

The C=S bond length of 1.681(3) Å in particular, as well as other bond lengths and angles, agrees with the literature values [8]. Selected bond lengths and angles are given in Table 1.

The triazole and furan rings are planar with deviation from the mean plane within 3σ except for N4 and C5 atoms, which deviate by 0.007(2) Å from the best plane. The S1 and C12 atoms show a displacement from the plane of the rings to which they are attached: −0.077(4) Å for S1 and 0.052(6) Å for C10.

The molecular structure of **1** is nonplanar. The average dihedral angle between the triazole and furan rings is 59.9(1)°. The corresponding dihedral angle between the triazole ring and the acetic acid substituent is 81.4(2). As evidenced by the results tabulated in Table 1, theoretical calculations show that the geometry in a very good agreement with the one observed experimentally in the crystal. Small

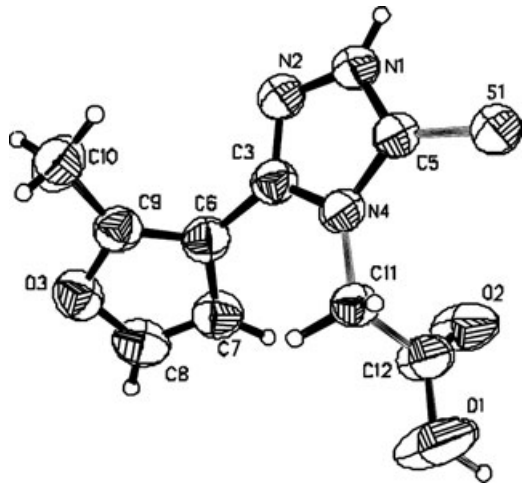

FIGURE 2 The molecular structure of **1** and the atom-numbering scheme. Ellipsoids for non-hydrogen atoms are drawn at the 50% probability level.

TABLE 1 Selected Bond Lengths (Å) and Torsional Angles (°) of **1**, Observed and Calculated for the NH and SH Tautomers

	Experiment	*NH*	*SH*
	Bond Lengths		
N1–N2	1.370(4)	1.360	1.372
N2–C3	1.302(4)	1.308	1.315
C3–N4	1.370(4)	1.385	1.384
N4–C5	1.362(4)	1.384	1.369
C5–N1	1.340(3)	1.355	1.309
C6–C7	1.437(4)	1.440	1.441
C7–C8	1.326(5)	1.355	1.356
C8–O3	1.364(4)	1.361	1.356
O3–C9	1.360(4)	1.356	1.358
C9–C6	1.353(4)	1.374	1.374
	Torsional Angles		
C9–C6–C3–N2	−59.2(4)	−40.4	−37.3
C9–C6–C3–N4	118.2(3)	138.2	140.9
C7–C6–C3–N2	123.1(4)	137.9	140.8
C7–C6–C3–N4	−59.6(4)	−43.4	−41.0
C3–N4–C11–C12	102.0(3)	99.4	102.4
C5–N4–C11–C12	−85.1(3)	−84.7	−84.5

deviations in these two dihedral angles (under 10°) can be due to crystal packing (described below).

In the crystal, molecules form tapes, which are parallel to the y axis (Fig. 3). Within the tapes, molecules are oriented "head to head" and are connected by N—H···S and C—H···O hydrogen bonds. The N1—H1n···S1 hydrogen bond links inversion-related molecules to dimers. The N1···S1 distance (3.256(3) Å) is shorter than the mean value of 3.44(1) Å [9]. Also, the N1—H1n···S1 angle is 170(3)° and is wider than the mean angle of 158(1)° (Table 2).

TABLE 2 Geometry of Intermolecular Hydrogen Bonds

D—H···A	*H···A (Å)*	*D···A (Å)*	*∠ (°)*
N1—H1n···S1[a]	2.40(3)	3.256(3)	170(3)
O1—H1o···N2[b]	2.13	2.909(4)	137
C11—H11b···O3[c]	2.48	3.439(4)	168

[a] $-x, 1-y, 1-z$.
[b] $x+1, 3/2-y, z+1/2$.
[c] $-x, 2-y, 1-z$.

The C—H···O hydrogen bonds, within the tapes, are methylene(C11)···furan(O3), whereas the neighboring tapes are linked by O1—H···N2 hydrogen bonds (Table 2). The crystal structure is further stabilized by the $\pi\cdots\pi$ stacking interactions between the inversion-related ($-x$, $2-y$, $1-z$) furan rings; the distance between centroids of furan rings is 3.525 Å. In addition, C—H···π (methylene(C11)···furan(C6): C11···C6 = 3.998(3), H11a···C6 = 3.30 Å, ∠ 130°, symmetry code: $x+1$, y, z) interaction is also observed.

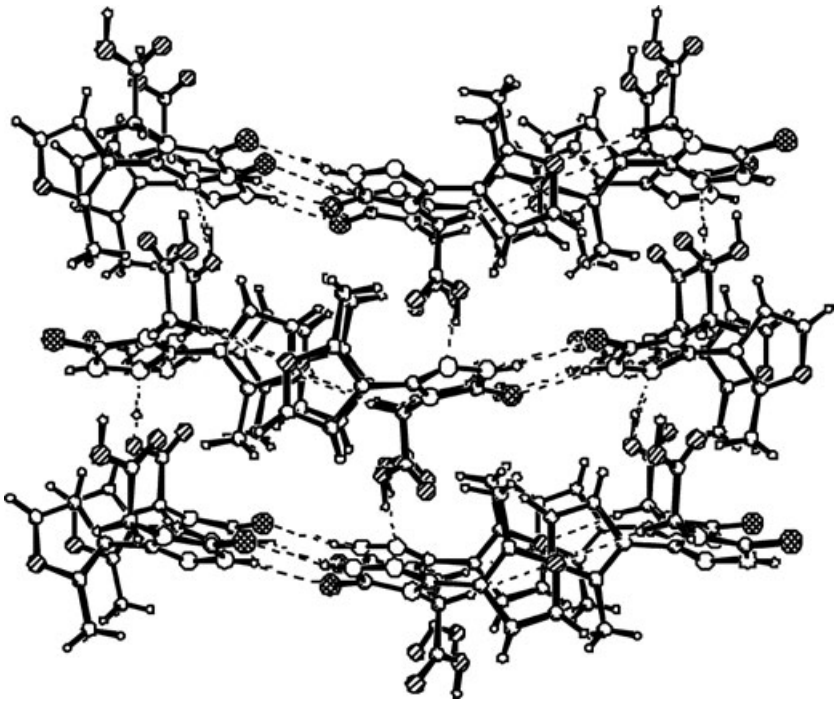

FIGURE 3 The packing arrangement of the molecules within the crystal; the view is along the *x* axis.

Vibrational Analysis

Infrared and Raman spectra for thione and thiol tautomers of **1**, predicted theoretically, are shown in Figs. 4 and 5, respectively. It should be kept in mind that theoretical calculations systematically overestimate the absolute position of the vibrational signals. The obtained frequencies should be, therefore, corrected. For the theory level used, the scaling factor is 0.9573 [10].

The comparison of the vibrational spectra for thione and thiol tautomers reveals that, not surprisingly, these spectra are fairly similar, and only small details are indicative of the actual form studied. In the IR spectrum, it is the intense signal at 1462 cm^{-1} (after scaling) that is indicative of the thione form. It corresponds to the bending of the hydrogen atom attached to N1 nitrogen atom in the plane of the triazole ring. It is predicted that the most intense signal in the spectrum agrees very well with the experimental result; the three most intense peaks obtained experimentally are observed at 1175.0, 1499.8, and 1744.0 cm^{-1}. As can be seen, the same triad is predicted theoretically at 1152.4, 1462.0, and 1798.8 cm^{-1}, the other two signals corresponding to bending and stretching vibrations are of the carboxyl group.

In the Raman spectra, it is only the signal at 2625.4 cm^{-1}, corresponding to the stretching mode of the S—H vibration, which could safely be used for the differentiation of the tautomeric forms. Thus, again not surprisingly, we concluded that in the vibrational spectra only the modes connected with the N1—H (IR-active) and S—H (Raman-active) vibrations could be used to distinguish the actual form of the studied compound. However, in the real system the molecule can interact with the environment, forming hydrogen bonds to the solvent or other molecules (e.g., in dimers). This will obviously change frequencies as well as intensities of the signals corresponding to the protons in question, rendering vibrational analysis not very useful for deciding the actual tautomeric form of the solution.

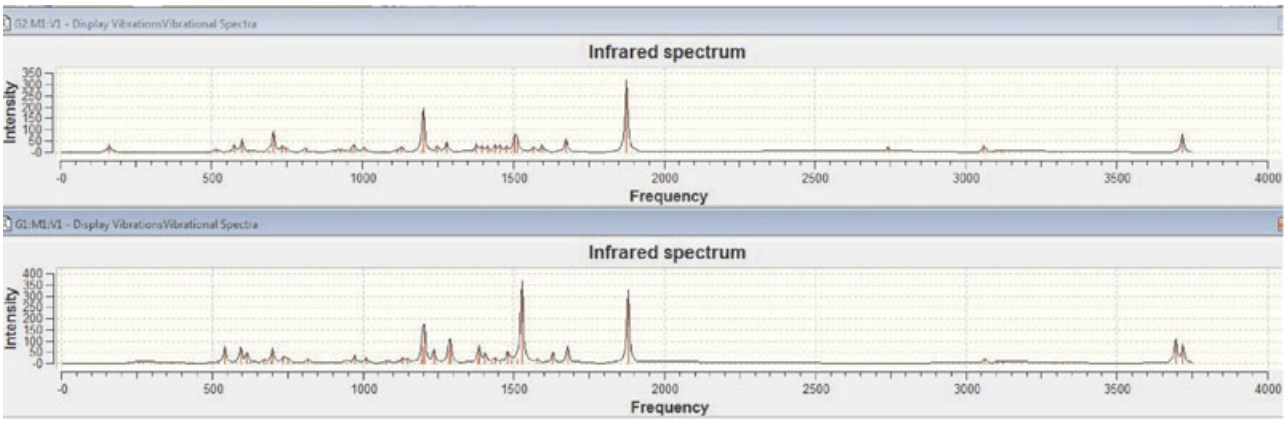

FIGURE 4 Theoretical IR spectra of SH (top) and NH (bottom) tautomers.

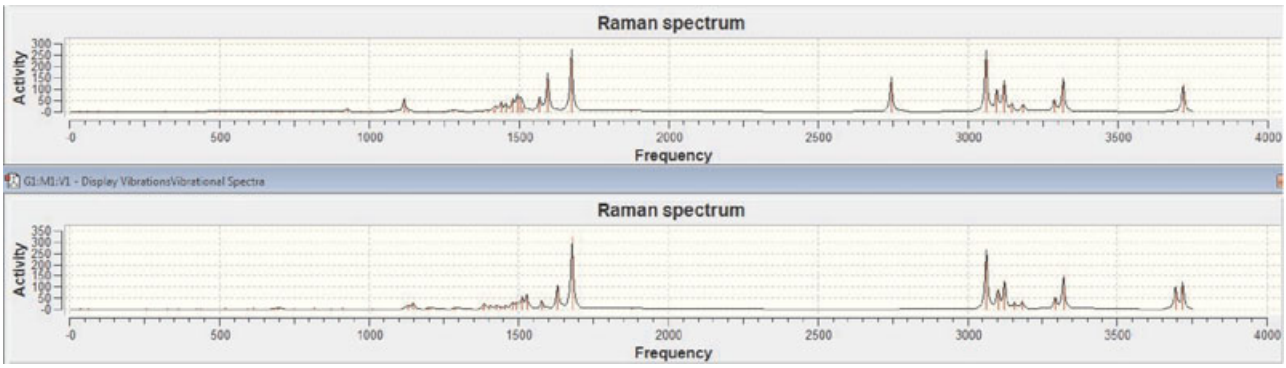

FIGURE 5 Theoretical Raman spectra of SH (top) and NH (bottom) tautomers.

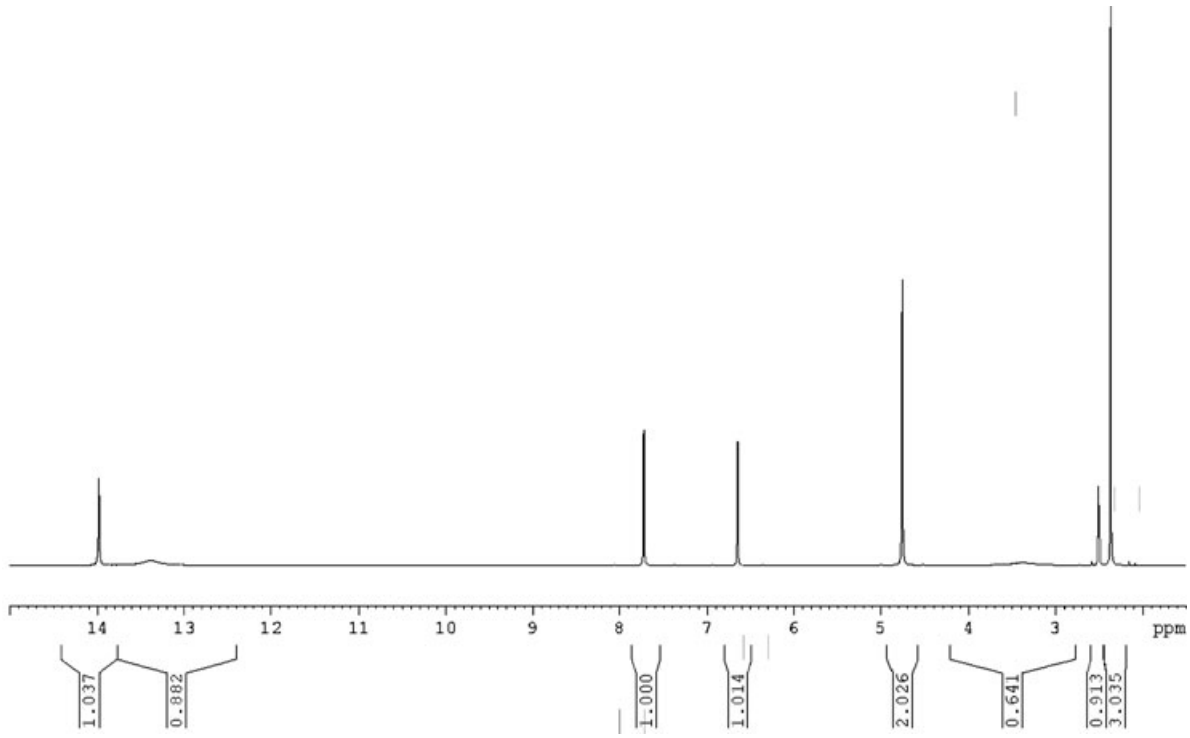

FIGURE 6 ^{1}H NMR spectrum of the NH tautomer in DMSO.

Discussion of NMR Spectra

The experimental ^{1}H NMR spectrum (Fig. 6) shows a sharp singlet at 14.0 ppm typical of the proton linked to N1, indicating the presence the thione tautomer. The comparison of this spectrum with theoretical predictions for both tautomers is given in Table 3.

This comparison indicates that theoretically predicted ^{1}H NMR spectrum proved inaccurate for the labile protons. The signals from the proton bonded to the N1 atom and from the proton in the carboxyl group were calculated to appear at 8.9 and 6.3 ppm, respectively. This is slightly improved when the continuum solvent model with DMSO parameters is used; both signals are shifted downfield to 9.1 and 10.8, respectively. However, the calculated chemical shifts are still about 4 ppm upshifted compared with the experimentally determined positions. It is worth noticing though that the assignment of signals corresponding to the other hydrogen atoms is quite good. Furthermore, as can be seen from the results reported in the last two sections, the differences between theoretical spectra predicted for both tautomers cannot be diagnostic of the actual form present in the solution, because the only difference is observed for the positions that are badly miscalculated by the theoretical approach. Experimentally such differentiation should be possible, because instead of the sharp signal at 14.0 ppm in the case of the NH tautomer one should see a broad signal at about 13.6 ppm, corresponding to the thiol proton, in the case of the SH tautomer. For the reported herein compound **1**, this signal would have significant overlap with the carboxylic proton, although its presence should be reflected in the integration.

TABLE 3 ^{1}H NMR Chemical Shifts (ppm) of **1**, Observed and Calculated for the NH and SH Tautomers

Atom	*Experimental NH*	*Theoretical NH*	*Theoretical SH*
N1H/S1H	14.0	8.9	5.1
O1H	13.4	6.3	6.4
C8H	7.7	7.8	7.8
C7H	6.7	7.0	6.8
$C11H_2$	4.8	4.9	4.9
$C10H_3$	2.4	2.8	3.0

We now discuss about ^{13}C and ^{15}N NMR spectra. As illustrated by the results presented in Table 4, in the theoretically predicted ^{13}C spectra of the tautomers the only signal that significantly differentiates NH and SH spectra are the one originating from the thiocarbonyl group. It is predicted to appear at 150.8 ppm in the thiol tautomer spectrum

TABLE 4 ^{13}C NMR Chemical Shifts (ppm) of 1, Observed and Calculated for the NH and SH Tautomers

Atom	Experimental NH	Theoretical NH	Theoretical SH
C5	168.4	170.4	170.1
C12	167.5	169.6	157.8
C9	153.8	157.5	151.0
C3	146.2	146.6	146.8
C8	142.5	142.4	141.6
C7	109.6	110.7	109.4
C6	106.5	109.1	109.4
C11	45.1	43.3	43.6
C10	12.5	10.3	10.0

and is shifted downfield to 169.5 ppm in the thione tautomer spectrum. This latter value agrees very well with the experimentally determined shift at 167.5 ppm. A good agreement between experimental and theoretical spectra for the NH tautomer suggests that this difference should be easily detectable and thus ^{13}C spectra should be useful in deciding which tautomeric form is present in the studied sample.

The experimental ^{15}N NMR spectra are not available, and, therefore, we restrict our discussion to the comparison of the calculated spectra for both tautomers. They are illustrated in Fig. 7.

As can be seen these spectra are significantly different (note the scale of the difference). The signal from N4 is predicted in the highest field at 186.8 and 174.5 ppm for NH and SH tautomers, respectively. The corresponding values for N2 are 293.0 and 356.6 ppm, respectively. These latter values seem sufficiently different to serve as a diagnostic tool to distinguish between the thione and thiol tautomers. Even more sensitive is the signal connected with the N1 atom; its chemical shift for the NH form is expected at 210.0 ppm and its counterpart in the spectrum of the SH tautomer at 344.0 ppm, allowing the fairly easy determination of the actual tautomeric form. Although the natural abundance of ^{15}N is low, the advent of high field NMR spectrometers allows for a relatively easy registration of a spectrum—in our experience an excellent nitrogen spectrum can be obtained under half an hour by using a 700-MHz spectrometer.

In summary, we analyzed structural and spectroscopic properties of **1**, which served as a well-defined tautomer with hydrogen atom attached to nitrogen. It was shown that vibrational analysis is not the best tool to tackle the problem of the actual tautomeric form in solution. Appearance of the bands at about 2600 cm^{-1}, connected with the S—H stretching mode, in the Raman spectra should be indicative of the thiol form, whereas high absorbance of the bands at about 1460 cm^{-1}, connected with the N—H bending mode, in the IR spectra points to the thione form of the studied compound. Within the NMR spectroscopic study, low-field signals in ^{1}H spectra, and especially lowfield signals in ^{15}N spectra should be the most informative ones regarding the tautomeric form of the studied mercapto-triazole derivative.

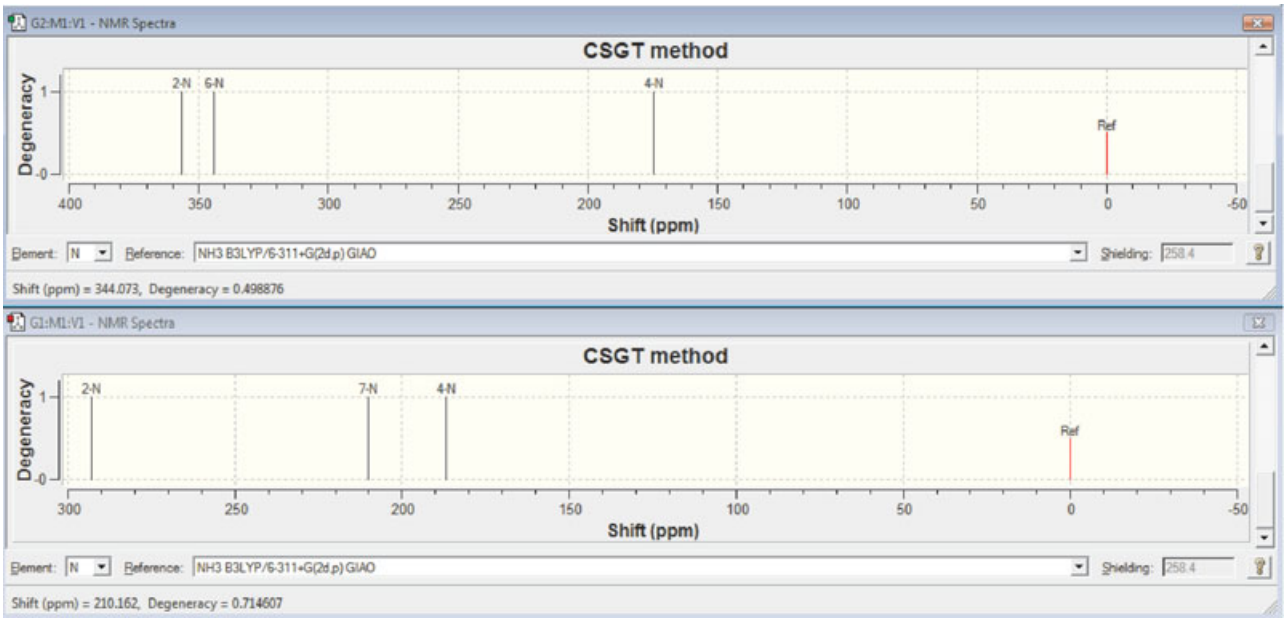

FIGURE 7 Theoretical ^{15}N NMR spectra of SH (top) and NH (bottom) tautomers.

EXPERIMENTAL

Material and Procedures

Melting points were determined in Fisher-Johns blocks and are presented without corrections. IR spectra (ν, cm^{-1}) were recorded in KBr using a Specord IR-75 spectrophotometer. ^1H and ^{13}C NMR spectra (δ, ppm) were recorded on a Bruker Avance 300 in DMSO-d_6 with TMS as an internal standard.

Synthesis of 4-Ethoxycarbonylmethyl-1-[(2-methyl-furan-3-yl)carbonyl]thiosemicarbazide. 2-Methyl-furan-3-carboxylic acid hydrazide (0.01 mol) and isothiocyanate (0.01 mol) were heated in an oil bath at 80°C for 12 h. The formed product was washed with diethyl ether to remove the unreacted isothiocyanate and then with hot water to remove the hydrazide residues. The product was dried and crystallized from ethanol.

Yield: 86%, mp 285–287°C; IR (KBr): 3362, 3268 (NH), 2975, 1446, 1293 (CH_3), 1759, 1665 (C=O), 1511, 1390 (C=S), 1191 (C—O—C) cm^{-1}; ^1H NMR (DMSO-d_6) δ: 1.17–1.22 (t, 3H, $J = 7.1$ Hz, $CH_2\underline{CH_3}$), 2.52 (s, 3H, furan CH_3), 4.06–4.13 (q, 2H, $J = 7.1$ Hz, $\underline{CH_2}CH_3$), 4.16–4.18 (d, 2H, $J = 5.6$ Hz, CH_2), 6.92–6.93 (d, 1H, $J = 2.0$ Hz, furan H), 7.55–7.56 (d, 1H, $J = 2.0$ Hz, furan H), 8.28, 9.52, 10.02 (3s, 3H, 3NH) ppm. Anal. calcd $C_{11}H_{15}N_3O_4S$ (C, H, N).

*Synthesis of 4-[3-(2-Methyl-furan-3-yl)-5-thioxo-1,2,4-triazolin-4-yl]acetic Acid (**1**).* The thiosemicarbazide derivative **1** (0.01 mol) was dissolved in 2% NaOH (10 mL) and refluxed for 2 h. After cooling the solution was neutralized with 3 M HCl. The solid formed was filtered, dried, and crystallized from ethanol.

Yield: 91%, mp 273–275°C; IR (KBr): 3470 (NH), 2947, 1387 (CH_3), 1779 (C=O), 1636 (C=N), 1568 (C—N), 1232 (C—O—C) cm^{-1}; ^1H NMR (DMSO-d_6) δ: 2.37 (s, 3H, furan CH_3), 4.76 (d, 2H, CH_2), 6.65–6.66 (d, 1H, $J = 2.0$ Hz, furan H), 7.72–7.73 (d, 1H, $J = 2.0$ Hz, 1H furan), 13.38 (s, 1H, OH), 13.98 (s, 1H, NH) ppm. Anal. calcd $C_9H_9N_3O_3S$ (C, H, N).

Crystal Structure Determination

Crystallographic analysis was made from single crystals formed from ethanol by slow solvent evaporation at room temperature. Diffraction data were collected on a KUMA KM4 diffractometer ($T = 293$ K, Cu Kα: $\lambda = 1.54178$ Å). Up to $\theta_{max} = 80.19°$, 2412 reflections were collected. Crystal structure was solved by direct methods (SHELXS-97 [11]) and refined by full-matrix least-squares on F^2 using the program SHELXL-97 [12]. The non-hydrogen atoms were refined anisotropically. The H atoms on N1 and O1 were located by the difference Fourier synthesis, whereas other H atoms were positioned geometrically. Final R indices for reflections with $I > 2\sigma(I)$ are $R_1 = 0.0706$, $wR_2 = 0.1819$ ($R_1 = 0.1020$, $wR_2 = 0.2116$ for all data).

Supplementary material has been deposited at the Cambridge Crystallographic Data Centre (deposition number CCDC 296379). These data can be obtained free of charge from The Cambridge Crystallographic Data Centre via www.ccdc.cam.ac.uk/data_request/cif.

Computational Methods

All calculations were carried out at the DFT level of theory using the hybrid B3PW91 functional [13]. The 6–31G(d) [14] basis set was employed. Molecular geometries were fully optimized in the gas phase. Vibrational analysis was carried out to confirm identity of the stationary points (3n-6 real vibrations), to calculate frequencies of normal modes, and to calculate Gibbs free energies at the temperature of 298 K and the pressure of 1 atm. As previously done in [15], NMR spectra were calculated using 6-311+G(2d,f) basis set [16]. NMR-shielding tensors were computed with the continuous set of gauge transformations method [17]. The IEF-PCM continuum solvation model [18] with parameters for DMSO was used to calculate the NMR spectra by using the GIAO approach [19] (data not shown).

ACKNOWLEDGMENTS

Piotr Paneth acknowledges the CNRS support.

REFERENCES

[1] (a) Prasad, A. R.; Rao, A. N.; Ramalingam, T.; Sattur, P. B. Indian J Chem, B 1986, 25, 776–778; (b) Holla, B. S.; Shivanda, M. K.; Akberali, P. M.; Baliga, S.; Safeer, S. Farmaco 1996, 51, 785–792; (c) Prasad, A. R.; Ramalingam, T.; Rao, A. B.; Diwan, P. V.; Sattur, P. B. Eur J Med Chem 1989, 24, 199–201; (d) Shouji, E.; Buttry, D. A. J Phys Chem B 1998, 102, 1444–1449; (f) Hipler, F.; Gil Girol, S.; Fischer, R. A.; Wöll, Ch. Mat-wiss u Werkstofftechn 2000, 31, 872–877; (g) Buynak, J.; Doppalapudi, V.; Rao, A.; Nidamarthy, S.; Adam, G. Bioorg Med Chem Lett 2000, 10, 847–851; (h) Renard, I.; Li, H.; Marsan, B. Electrochim Acta 2003, 48, 831–844.

[2] (a) Katritzky, A. R.; Wang, Z.; Offerman, R. J Heterocyclic Chem 1990, 27, 139–142; (b) Raper, E. S. Coord Chem Rev 1996, 153, 199–255; (c) Raper, E. S. Coord Chem Rev 1997, 165, 475–567; (d) Katritzky, A. R.; Borowiecka, J.; Fan, W. Q.; Brannigan, L. H. J Heterocycl Chem 1991, 28, 1139–1141.

[3] (a) Guziec, L. J.; Guziec, F. S., Jr. J Org Chem 1994, 59, 4691–4692; (b) Taurog, A.; Dorris, M. L.; Guziec, L. J.; Guziec, F. S., Jr. Biochem Pharm 1994, 48, 1447–1453.
[4] (a) Raper, E. S. Coord Chem Rev 1994, 129, 91–156; (b) Creighton, J. R.; Gardiner, D. J.; Gorvin, A. C.; Gutteridge, C.; Jackson, A. R. W.; Raper, E. S.; Sherwood, P. M. A. Inorg Chim Acta 1985, 103, 195–205; (c) Oughtred, R. E.; Raper, E. S.; Nowell, I. W. Acta Crystallogr, Sect C: Cryst Struct Commun 1985, 41, 758–760; (d) Atkinson, E. R.; Gardiner, D. J.; Jackson, A. R. W.; Raper, E. S. Inorg Chim Acta 1985, 98, 35–41; (e) Turan-Zitouni, G.; Kaplancikli, Z. A.; Erol, K.; Kiliç, F. S. Il Farmaco 1999, 54, 218–223; (f) Roy, G.; Mugesh, G. J Am Chem Soc 2005, 127, 15207–15217; (g) Roy, G.; Das, D.; Mugesh, G. Inorg Chim Acta 2007, 360, 303–316; (h) Coyanis, E. M.; Della Vedova, C. O.; Haas, A.; Winter, M. J Fluorine Chem 2002, 117, 185–192.
[5] (a) Zamani, K.; Faghihi, K.; Tofighi, T.; Shariatzadeh, M. R. Turk J Chem 2004, 28, 95–100; (b) Sarhan, A. A. O. Monatsh Chem 2001, 132, 753–763; (c) Kothari, P. J.; Kishore, V.; Stenberg, V. I.; Parmar, S. S. J Heterocyclic Chem 1978, 15, 1101–1104; (d) Roy, G.; Nethaji, M.; Mugesh, G. J Am Chem Soc 2004, 126, 2712–2713; (e) Koparir, M.; Cetin, A.; Cansiz, A. Molecules 2005, 10, 475–480.
[6] Fu, A.; Li, H.; Du, D. J. Mol Struct Theochem 2006, 767, 51–60.
[7] Siwek, A. PhD Thesis, Medical Academy, Lublin, Poland, 2007.
[8] (a) Öztürk, S.; Akkurt, M.; Cansız, A.; Koparır, M.; Sekerci, M.; Heinemann, F. W. Acta Crystallogr, Sect E: Struct Rep Online 2004, 60, o425–o427; (b) Öztürk, S.; Akkurt, M.; Koparır, M.; Cansız, A.; Sekerci, M.; Heinemann, F. W. Acta Crystallogr, Sect E: Struct Rep Online 2004, 60, o2368–o2370.
[9] Allen, F. H.; Bird, C. M.; Rowland, R. C.; Raithby, P. R. Acta Crystallogr, Sect B: Struct Sci 1997, 53, 680–695.
[10] Scott, A. F.; Radom, L. J Phys Chem 1996, 100, 16502–16513.
[11] Sheldrick, G. M. SHELXS-97, Program for Crystal Structure Solution; University of Göttingen: Göttingen, Germany, 1997.
[12] Sheldrick, G. M. SHELXL-97, Program for the Refinement of Crystal Structures from Diffraction Data; University of Göttingen: Göttingen, Germany, 1997.
[13] (a) Becke, A. D. Phys Rev A 1988, 38, 3098–3100; (b) Becke, A. D. J Chem Phys 1993, 98, 5648–5652; (c) Perdew, J. P.; Chevary, J. A.; Vosko, S. H.; Jackson, K. A.; Pederson, M. R.; Singh, D. J.; Fiolhais, C. 1992, Phys Rev B 46, 13584–13591.
[14] (a) Hariharan, P. C.; Pople, J. A. Theor Chim Acta 1973, 28, 213–222; (b) Francl, M. M.; Pietro, W. J.; Hehre, W. J.; Binkley, J. S.; Gordon, M. S.; DeFrees, D. J.; Pople, J. A. J Chem Phys 1982, 77, 3654–3665.
[15] Błazewska, K.; Paneth, P.; Gajda, T. J Org Chem 2007, 72, 878–887.
[16] Krishnan, R.; Binkley, J. S.; Seeger, R.; Pople, J. A. J Chem Phys 1980, 72, 650–654.
[17] (a) Keith, T. A.; Bader, R. F. W. Chem Phys Lett 1992, 194, 1–8; (b) Cheeseman, J. R.; Frisch, M. J.; Trucks, G. W.; Keith, T. A. J Chem Phys 1996, 104, 5497–5509.
[18] Cancès, M. T.; Mennucci, B.; Tomasi, J. J Chem Phys 1997, 107, 3032–3041.
[19] Ruud, K.; Helgaker, T.; Bak, K. L.; Jørgensen, P.; Jensen, H. J. A. J Chem Phys 1993, 99, 3847–3859.